Heliyon 9 (2023) e17600

Contents lists available at ScienceDirect

Heliyon

journal homepage: www.cell.com/heliyon

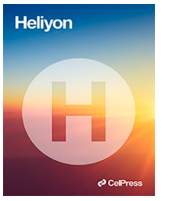

Knockdown of FUT11 inhibits the progression of gastric cancer via the PI3K/AKT pathway

Wenpeng Cao [a,1], Zhirui Zeng [b,1], Jinzhi Lan [b], Yushi Yang [c], Min Lu [d,**], Shan Lei [b,*]

[a] Department of Anatomy, School of Basic Medicine, Guizhou Medical University, Guiyang 550009, Guizhou, China
[b] Department of Physiology, School of Basic Medicine, Guizhou Medical University, Guiyang 550009, Guizhou, China
[c] Department of Pathology, Affiliated Hospital of Guizhou Medical University, Guiyang 550009, Guizhou, China
[d] Department of Gastroenterology, Zhujiang Hospital, Southern Medical University, Guangzhou, 510000, Guangdong, China

ARTICLE INFO

Keywords:
Gastric cancer
Fucosyltransferase family
FUT11
COL6A3
Proliferation

ABSTRACT

Gastric cancer (GC) is a common and highly malignant tumor of the digestive tract. Members of the focused fucosyltransferase (FUT) family participate in the advancement of various types of cancer. However, research of FUT family members in the progression of GC known to be limited. The purpose of the research was to determine the function of important affiliates of the FUT family in GC and to explore its impacts on the proliferation and migration of GC cells and molecular mechanisms. For the study, fucosyltransferase11 (FUT11) was confirmed to be the only affiliate of the FUT family that was upmodulated in GC tissues and linked to poor survival according to GEPIA data. Furthermore, compared with adjacent noncancerous tissues, the expression of FUT11 was increased in GC tissues. The elevated FUT11 expression suggested that the overall survival (OS) rate of GC is low. Inhibition of FUT11 significantly reduced the proliferation and migration and suppressed the PI3K/AKT pathway by down-regulated collagen type VI alpha 3 chain (COL6A3) in GC cells. The present study has demonstrated that reinstating the expression of COL6A3 in gastric cancer (GC) cells can counteract the inhibitory impact of FUT11 knockdown on the proliferation and migration of GC cells. In conclusion, FUT11 may serve as a novel biomarker for GC, as it modulates GC cell proliferation and migration through the PI3K/AKT signaling pathway.

1. Introduction

Gastric cancer (GC) has been reported to be the third commonest malignancy and second main contributor to tumor associated mortality globally [1]. It is most common for GC patients to be diagnosed with advanced disease or distant metastatic disease due to the absence of symptoms in the early stages [2]. Although advancements in diagnosis and treatment strategies have been made over the past several decades, the prognosis for advanced-stage patients remains grim [3]. Pathogenic and metastatic mechanisms of GC are complex and multifactorial, posing a major obstacle to patient survival [4]. The identification of key molecular events underlying GC progression and metastasis is therefore crucial for improving diagnosis and prognosis.

* Corresponding author. School of Basic Medicine, Guizhou Medical University, Dongqing Road, Guiyang, Guizhou 550009, PR China.
** Corresponding author. Zhujiang Hospital, Southern Medical University, Guangzhou, 510000, Guangdong, China.
E-mail addresses: Lumin2009amy@163.com (M. Lu), 1109974497@qq.com (S. Lei).
[1] Equal contribution.

https://doi.org/10.1016/j.heliyon.2023.e17600
Received 1 March 2023; Received in revised form 17 June 2023; Accepted 22 June 2023
Available online 7 July 2023

List of abbreviations

GC	Gastric cancer
OS	Overall Survival
COL6A3	collagen type VI alpha 3 chain
FUT11	fucosyltransferase 11
ATCC	American Type Culture Collection
CCK-8	Cell count kit-8
IHC	Immunohistochemical staining

Thus far, thirteen FUT genes of the fucosyltransferase (FUT) family have been identified in the human genome, FUT1 to 11, protein O-fucosyltransferase1 (POFUT1), and protein O-fucosyltransferase2 (POFUT2), respectively [5]. Mutation of FUT1 to 7 increased the occurrence risk of gastric cancer [6]. By inhibiting FUT4 transcription, myogenic differentiation 1 (MyoD1) suppressed GC cell migration and invasion [7]. FUT3 and FUT5 increased the adhesion capacities of gastric cancer cells [8]. POFUT1 was shown to be positively associated with the cell cycle and the cell carcinoma process, suggesting that it might be used as a biomarker in GC [9]. Herein, Therefore, it is essential to further investigate the role of the FUT family in the pathogenesis of gastric cancer.

The objective of the study was to investigate the participation of the FUT family in gastric cancer (GC), as well as their molecular mechanism and function in GC cell proliferation and mobility. The results of biological function experiments and bioinformatic analysis revealed that the expression of FUT11 was significantly upregulated in GC tissues and was an independent prognostic factor for unfavorable outcomes. Inhibition of the PI3K/AKT pathway through FUT11 knockdown led to a reduction in GC cell growth and motility. These findings suggest that FUT11 may serve as a novel and valuable biomarker for GC diagnosis.

2. Materials and methods

2.1. Cell culture

GC cell lines MKN-28, HGC-27, KATO-3, MKN-7, AGS and normal GES-1 gastric mucosa epithelium cell line were procured from the ATCC (American Type Culture Collection, USA). By STR identification, cell line was authenticated. Both of them were grown in RPMI-1640 medium (Gibco, USA) comprising of 10% fetal bovine serum (FBS; BI, Israel) at a temperature of 37 °C with a 5% CO_2 concentration. FUT11 short hairpin RNAs (shRNAs) and negative lentivirus (NC) were obtained from GeneCopoeia (Guangzhou). Vector and plasmid comprising of the CDS sequence of the COL6A3 gene were procured from GeneCopoeia (Guangzhou, China). The sequence of sh1- FUT11 was GGUGGUGUUGGUCCUUCUA; and the sequence of sh2-FUT11 was GGUGCUCAGUGUCUGUGCA; the sequence of sh-scramble was UUCUCCGAACGUGUCACGU.

2.2. GEPIA data analysis

FUT family expression in GC and adjacent tissues were retrieved and analyzed using the GEPIA database. $|\text{LogChange}|>1$ and $P < 0.05$ were set as significance thresholds. In order to differentiate between the low and high expression levels of genes in GC tissues, median gene expression values were used as a cut-off value. An analysis of the association between mRNA expression and patient prognosis was performed using Kaplan-Meier curves [10].

2.3. RNA sequencing

As part of the extraction procedure, total RNA was extracted from samples using the TRIzol reagent (ThermoFisher, USA) provided by ThermoFisher. RNA samples with a RIN number greater than 7.0, as determined by a Bioanalyzer 2100 and RNA 6000 Nano LabChip Kit (Agilent, CA, USA), were utilized to construct sequencing libraries. Reverse transcription was carried out using SuperScriptTM II Reverse Transcriptase (Invitrogen, USA), and mRNA was fragmented into short fragments after purification. The final library had cDNA inserts with an average length of 300 ± 50 bp. The cDNA was sequenced using Illumina NovaseqTM 6000 (LC-Bio Technology, Ltd., Hangzhou, China) following the vendor's protocol. The count data were analyzed using the EdgeR package after high-quality clean reads were obtained and batch normalization was performed. $P < 0.05$, and $\text{LogFC} \geq 2$ were used as test criteria for differentially expressed genes.

2.4. Cell count kit-8 (CCK-8) assay

A density of 4×10^3 AGS and MKN-28 cells per well, with eight parallel wells per group, was applied in 96-well plates. 24 and 48 h of culture in the incubator followed by 1 h incubation in fresh medium containing 10% CCK-8 solution (Boster, Wuhan, China) was conducted. An automatic multifunctional enzyme labeler (Varioskan LUX, Thermo Fisher Scientific, USA) was used to measure absorption at a wavelength of 450 nm.

2.5. Colony formation assay

An aggregate of 1.5×10^3 AGS and MKN-28 cells were set into the six-well plates. After culturing for a duration of 10 days, these cells were immobilized for 15 min using 4% paraformaldehyde , followed by staining with 0.1% crystal violet at 20 min (Servicebio, Wuhan, China). Finally, camera was used to record the condition of cell colonies in per plate.

2.6. 5-Ethynyl-2 (EDU) assay

A BeyoClick™ EDU-488 cell proliferation detection kit (Beyotime Biotechnology, Hangzhou, China) was utilized to carry out EDU assay as per the instructions stipulated by the manufacturer. Succinctly, an aggregate of 5×10^4 AGS and MKN-28 cells was cultured in a confocal dish. Then, cells were incubated for 2 h with 50 μM EDU reagent. Following phosphate-buffered saline (PBS) wash, fixing of the cells was done with 4% paraformaldehyde for 30 min before being incubated with Apollo staining reaction liquid for an additional 30 min to identify positive cells. After being stained with 4,6-diamino-2-phenylindole to detect the nucleus, a fluorescence microscope was utilized to observe the immunofluorescence at 488 nm.

2.7. Quantitative real-time PCR (RT-qPCR)

TRIzol reagent was utilized to extract total RNA from the cultivated cells, and RevertAid First Strand cDNA Synthesis Kit (Thermo Scientific, Waltham, MA, USA) was used to synthesize complementary DNAs (cDNAs) with 2 μg total RNA. RT-qPCR was conducted to identify the specific gene expression differences utilizing Aceq Universal SYBR qPCR Master Mix (Vazyme, Nanjing, China) on Roche LightCycler480 (Roche, Shanghai, China). For this experiment, β-actin served as a loading control. The relative expression of target genes was measured utilizing the $2^{-\Delta\Delta}$Ct method. The primers used in the present study were shown as follows:

FUT11 Forward: 5′-ATGCCGAACAATCACTCCGT-3′
FUT11 Reverse: 5′-AGATCTCCTTAGCTCCGCCA-3′
COL6A3 Forward: 5′-ATGAGGAAACATCGGCACTTG-3′
COL6A3 Reverse: 5′-GGGCATGAGTTGTAGGAAAGC-3’;
β-actin Forward: 5′-TCAGAAGGATTCCTATGTGGGCGA-3′,
β-actin Reverse: 5′-TTTCTCCATGTCGTCCCAGTTGGT-3’.

2.8. Western blot

The total proteins of cells was extracted by a radioimmunoassay precipitation lysis buffer containing 1% phenylmethylsulfonyl fluoride lysis buffer (Servicebio, Wuhan, China). Protein concentrations of samples were determined in a bicinchoninic acid method (Solarbio, Beijing, China). The sodium dodecyl sulphate polyacrylamide gels (Meilune, Dalian, China) were utilized to isolate proteins, which were subsequently moved onto the polyvinylidene fluoride membranes (Thermo Scientific, USA). Following the use of skimmed milk powder to block the membranes (Beyotime Biotechnology, Suzhou, China), they were subjected to incubation with primary antibodies, containing FUT11 (1:1000; Proteintech, China), COL6A3 (1:1000; Abcam, USA), PI3K (1:1000; ABclonal, China), AKT (1:1000; ABclonal, China), p-AKT (1:1000; ABclonal, China), PTEN (1:1000; ABclonal, China), mTOR (1:1000; CST, USA), p-mTOR (1:1000; CST, USA)and β-actin (1:5000; ABclonal, China), for 24 h at 4 °C. After washing thrice using Tris-buffered saline comprising of 0.1% Tween-20, the membranes were subsequently subjected to the secondary antibody. Lastly, visualization of the bands was done by an enhanced chemiluminescence reagent. The ACTB was used as the control for calculating relative protein expression.

2.9. Wound healing assay

MKN-28 and AGS cells (5×10^5 GC cells/well) was placed in the six-well plates. 200 μL spearhead was employed to generate a wound in a monolayer cell. This was followed by washing twice with PBS to eliminate the floating cells and replacing the fresh medium. The healing conditions of the wound were recorded from 0 to 24 h in an optical microscope (magnification times, 40 ×).

2.10. Transwell assay

AGS and MKN-28 cells (1×10^5 GC cells/well) were resuspended in 300 μl FBS-free DMEM and introduced in the top transwell chambers (Corning, USA) which pre-coated a matrigel (ThermoFisher Scientific, USA), whereas 700 μl DMEM medium comprising of 10% FBS was set in the bottom transwell chambers. After 24h, immobilization of the invaded cells was done followed by staining for 20 min with 0.5% crystal violet. Finally, an inverted microscope was used to photo the invasive cells in the chambers. The numbers of cells in five random fields (up, down, left, right, middle) of each chamber was counted.

2.11. In vivo assay

For subcutaneously injected model, total 10 female BALB/c nude mice were obtained from the animal central of Guizhou Medical University (Guizhou, China). After adaptive feeding, total 2×10^6 MKN-28 cells with FUT11 knockdown and negative control cells were subcutaneously injected into upper-right flank of BALB/c mice (n = 5 in each group). The health status of mice was monitored per

day, while the tumor volume was detected per week. The tumor volume was monitored once a week and determined as followed: (mm^3) = (Long × Width [2])/2. After 4 weeks, all mice were euthanasia and the tumor tissues were extracted in order to detect the expression of Ki67 and PCNA using immunohistochemical staining.

2.12. Immunohistochemical staining (IHC)

Prior to IHC, the tumor tissues were immobilized, dried, and implanted in paraffin, the tumor tissue specimens were stripped into 3 μm samples to store. In IHC process, specimens were first deparaffinized and rehydrated using xylene and alcohols, respectively. After restoring the antigen with the sodium citrate reagent, the tissues were washed thrice by PBS ensued by blocking with H_2O_2 and BSA (Thermo Scientific, USA). Then, incubation of the samples was done with the primary anti-FUT11 antibody (1:100; Proteintech, China), anti-COL6A3 antibody (1:100; Abcam, USA), anti-Ki67 antibody (1:100; Proteintech, China) and anti-PCNA antibody (1:100; Proteintech, China) for 24 h at 4 °C. On the second day, staining of the sections was done with HRP-conjugated goat anti-rabbit secondary antibodies (ABclonal, Wuhan, China) for 2 h. After washing thrice by PBS, the tissues were subjected to incubation with the DAB (Beyotime Biotechnology, Suzhou, China) and hematoxylin, immune signals were detected by an orthophoto microscope.

2.13. Data analysis

SPSS 22.0 software (IBM Corp., USA) was utilized to analyze all the data in this research. To examine variations across multiple cohorts, ANOVA with Bonferroni's post hoc test was employed. T-tests were utilized to examine variations between two cohorts. *P < 0.05 was determined to be the threshold for statistical significance.

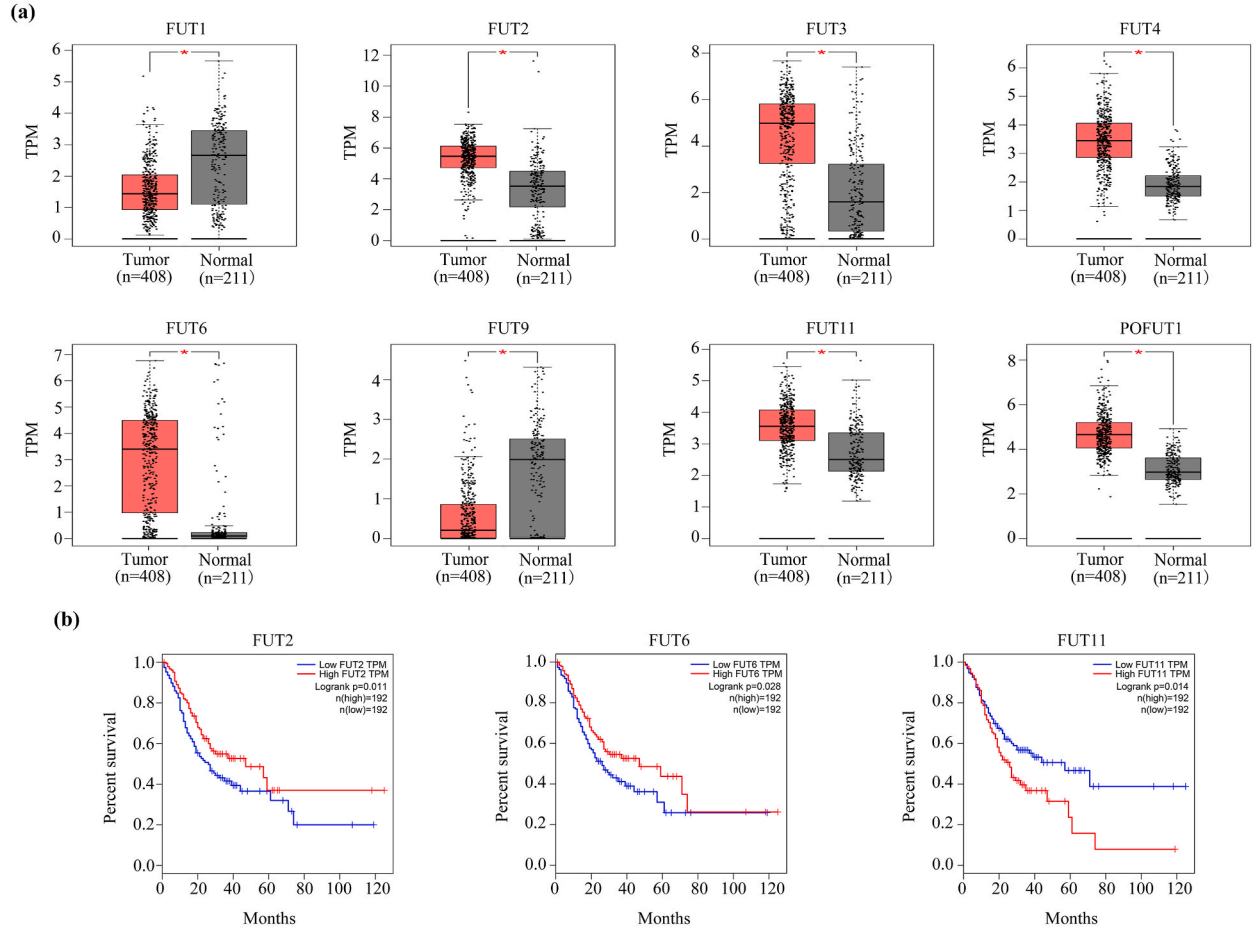

Fig. 1. The expression of members in FUT family and overall survival rate in GC tissues (GEPIA). (a) The expression of FUT2, FUT3, FUT4, FUT6, FUT11 and POFUT1 in GC tissues were significantly elevated, while the expression of FUT1 and FUT9 were significantly reduced. The p-value was set at 0.05. (b) The high expression of FUT2 and FUT6 was associated with a longer overall survival rate, while FUT11 significantly associated with a lower overall survival rate in GC. *P < 0.05.

3. Results

3.1. Role of FUT11 as an important member of the FUT family in GC

Previous studies have shown that affiliates of the FUT family are disordered in a variety of cancers [11–13]. Further, we investigated the potential role of the FUT family in gastric cancer (GC). Utilizing bioinformatics analysis of TCGA and GTEx data through GEPIA, we observed that FUT2, FUT3, FUT4, FUT6, FUT11, and POFUT1 exhibited increased expression in GC, while FUT1 and FUT9 expression was decreased (Fig. 1a). Furthermore, we found that elevated FUT2 expression and FUT6 expression were associated with greater overall survival (OS) rate in GC, whereas FUT11 expression was significantly associated with reduced OS in GC (Fig. 1b). FUT11 was found to be increasingly expressed in GC and closely related to a poor prognosis, so it will be further studied.

3.2. FUT11 increasingly expressed in GC tissues and exhibited major clinical significance

The FUT11 expression in GC tissues and adjacent noncancerous tissues was subsequently investigated, the results of IHC illustrated that the expression of FUT11 was higher in GC tissues than that in normal tissues (Fig. 2a–b). We conducted ROC analysis based on the protein levels identified by IHC. The findings demonstrated that FUT11 has a significant diagnostic value in GC (Fig. 2c). GC patients were classified into low and high expression cohorts based on the median expression value. The patients in the high expression cohort had poor survival compared with those in the low expression cohort (hazard ratio = 2.746, 95% confidence interval = 1.02–7.39; Fig. 2d). The RT-qPCR was used to determine the expression of FUT11 in GC cell lines (AGS, HGC-27, KATO-3, MKN-7, and MKN-28), and FUT11 expression was relatively high in AGS and MKN-28 (Fig. 2e).

3.3. Knockdown of FUT11 reduced the GC cell proliferation and mobility

Given that FUT11 is overexpressed in CCA tissues and cell lines, we further investigated the role of FUT11 in GC. Two shRNAs targeting FUT11 were synthesized and subsequently transfected into AGS and MKN-28 cell lines, resulting in significant silencing effects in both cell lines (Fig. 3a–b). CCK-8 assay demonstrated that the inhibition of FUT11 led to a reduction in the growth of AGS and MKN-28 cells after 24 and 48 h (Fig. 3c). Furthermore, the suppression of FUT11 expression resulted in a decrease in the colony-forming capacity of AGS and MKN-28 cells (Fig. 3d–e). Similarly, EDU assay revealed a decrease in the number of EdU-positive cells (red) upon FUT11 knockdown (Fig. 3f–g). Furthermore, flow cytometry showed that knockdown of FUT11 significantly increased the proportion of apoptosis in AGS and MKN-28 cells (Fig. 3h). Moreover, the wound healing assay and transwell assay revealed that FUT11 inhibition obviously decreased the migration (Fig. 4a–b) and invasion (Fig. 4c–d) of AGS and MKN-28 cells.

3.4. Knockdown of FUT11 reduced the GC cells proliferation in vivo

The effects of FUT11 knockdown *in vivo* was also determined. MKN-28 cells transfected with FUT11 shRNAs and negative control were injected subcutaneously into the nude mice. Compared to the control group, mice injected with FUT11-knockdown cells displayed significantly decreased tumor volume and weight (Fig. 5a–c). Altered rates of cell proliferation are one of the hallmarks of tumour progression, and therefore, assessment of this feature may be useful in predicting patient prognosis. Proliferating cell nuclear

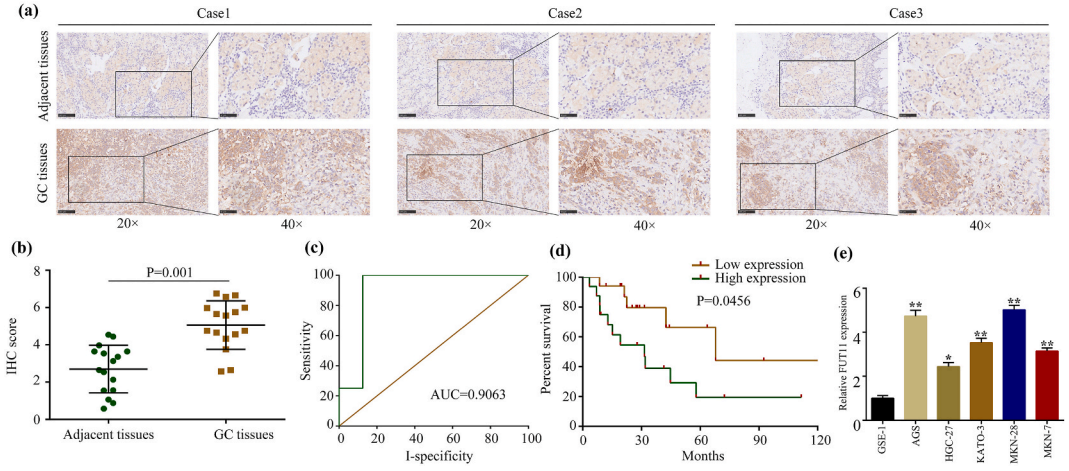

Fig. 2. FUT11 was up-regulated in GC tissues. (a) Immunohistochemical assay was used to detect the expression of FUT11 in adjacent tissues and GC tissues. (b)Statistical plot of immunohistochemical of assay. (c) ROC analysis for FUT11 based on immunohistochemical score. (d) Kaplan survival analysis for the high expression and low expression FUT11 group. (e). RT-qPCR analysis of relative expression levels of FUT11 in GC cell lines and GES-1 cells.*, $P < 0.05$, **, $P < 0.01$.

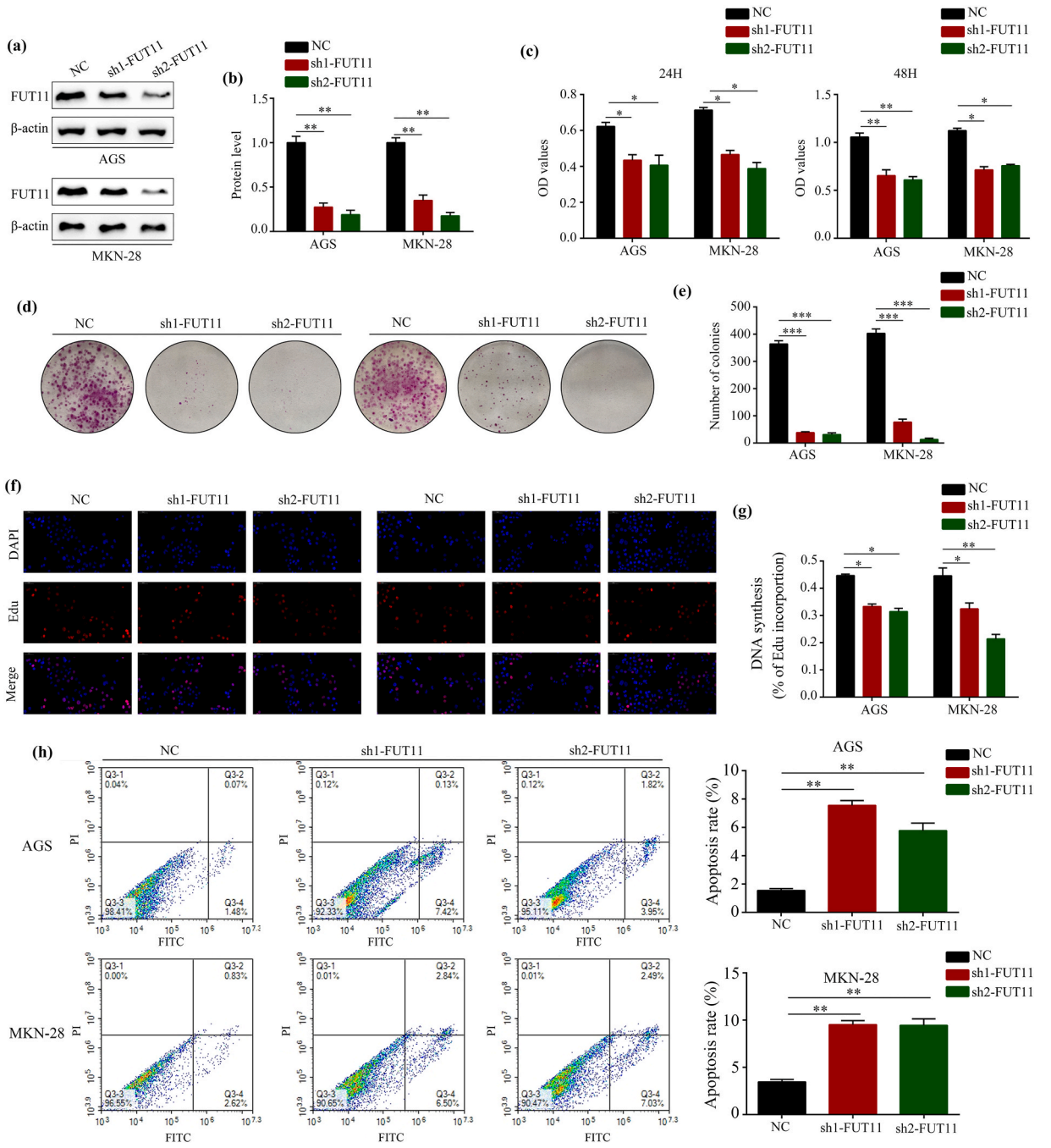

Fig. 3. Knockdown of FUT11 decreased the GC cells proliferation. (a) Western blot was used to detect the expression of FUT11 in FUT11 knockdown group and normal control (NC) group cell. (b) Statistical plot of Western blot of assay. (c) CCK-8 was used to detect the proliferation of FUT11 knockdown group and NC group cell. (d) Colony formation was used to detect the colony formation ability of FUT11 knockdown group and NC group cell. (e) Statistical plot of colony formation of assay. (f) EDU assay was used to detect the EDU-incorporating live cells of FUT11 knockdown group and NC group cell. (g) Statistical plot of EDU assay. (h) Flow cytometry was used to detect the percentages of apoptosis of FUT11 knockdown group and NC group cell. **, $P < 0.01$, ***, $P < 0.001$.

antigen (PCNA) and marker of proliferation Ki-67 (Ki67) is a nuclear protein and marker of cell proliferation [14,15]. Also, immunohistochemistry revealed that knockdown of FUT11 triggered a reduction of KI67 and PCNA protein expression in excised tumor tissues (Fig. 5d).

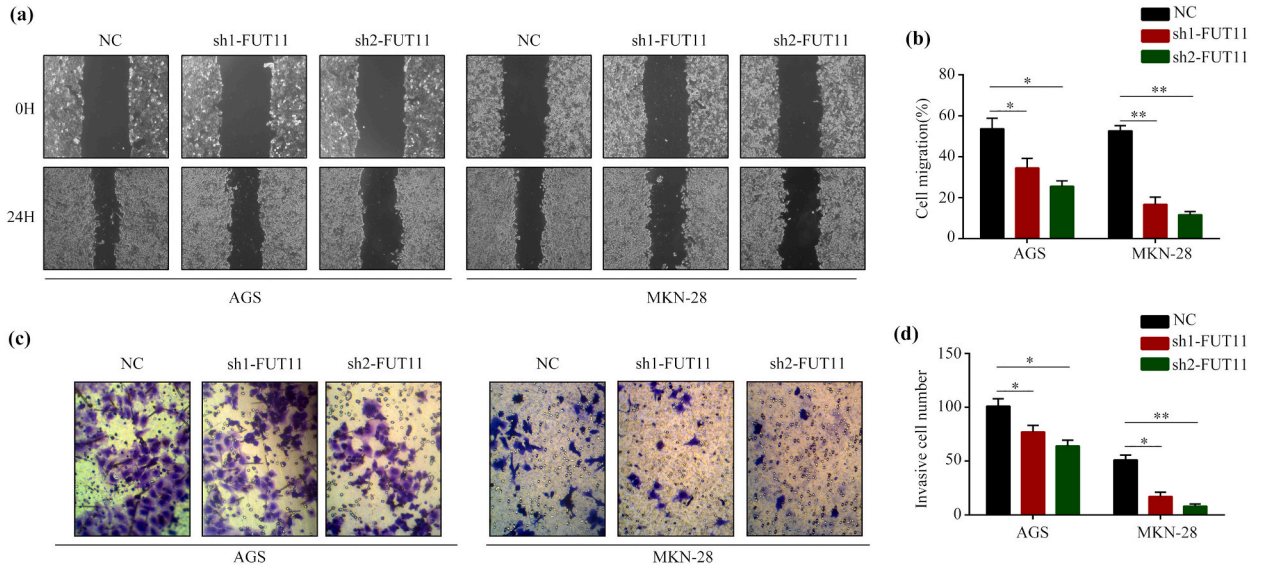

Fig. 4. Knockdown of FUT11 inhibited the GC cells mobility. (a) Wound healing assay was used to detect the migration of FUT11 knockdown group and negative control (NC) group cell. (b) Statistical plot of wound healing of assay. (c) Transwell assay was used to detect the invasion of FUT11 knockdown group and NC group cell. (d) Statistical plot of transwell assay of assay. *, $P < 0.05$; **, $P < 0.01$.

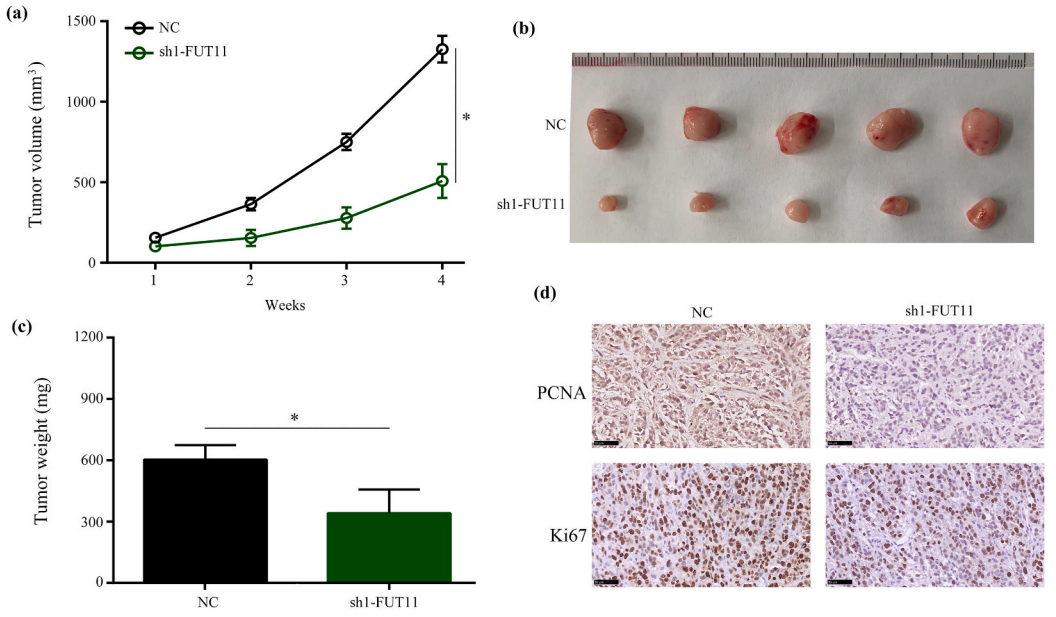

Fig. 5. Knockdown of FUT11 suppressed the proliferation of MKN-28 cells *in vivo*. (a) The proliferate rate of tumor tissues with FUT11 knockdown and negative control. (b) Typical image of tumor tissues in negative control group and FUT11 knockdown group. (c) The mean weight of tumor tissues with FUT11knockdown and negative control. (d) Typical IHC staining images showing Ki67 and PCNA expression in transplanted tumors under different experimental conditions. *, $P < 0.05$.

3.5. FUT11 suppression substantially reduced the PI3K/AKT pathway in GC cells

Further, by undertaking a bioinformatics analysis of the data retrieved from the GTEx and TCGA datasets, we discovered that COL6A3 was highly expressed in GC (Fig. 6a), In addition, according to data from GC tissues in the TCGA database, we observed that FUT11 was co-expressed with COL6A3 (Fig. 6b). By Pearson correlation analysis, the mRNA and protein level of FUT11 in GC tissues was positively correlated with COL6A3 expression with statistical significance (Fig. 6c–d). Western blotting showed that inhibiting FUT11 significantly reduced the expression of COL6A3 (Fig. 6e–f). Taken together, these findings showed that inhibiting the

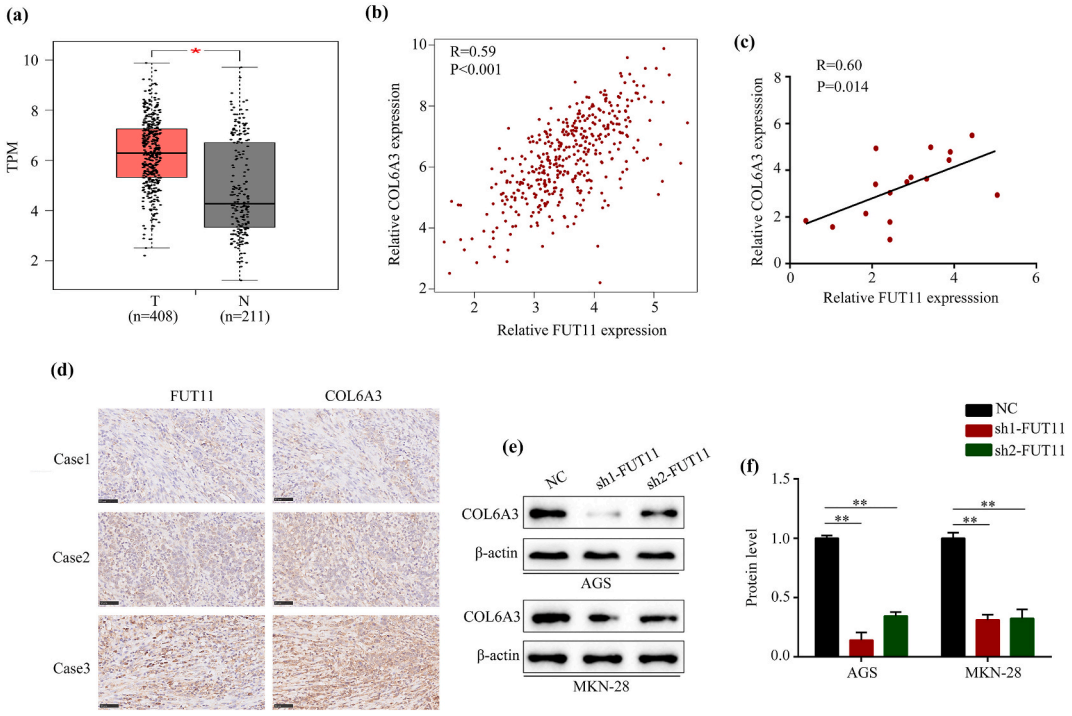

Fig. 6. Knockdown of FUT11 inhibited the expression of COL6A3. (a)The expression of COL6A3 were significantly elevated in GC tissues. (b–d) The co-expression relationship between FUT11 and COL6A3 in TCGA GC tissues and our GC tissues. (e) The expression of COL6A3 in negative control group and FUT11 knockdown cell. *, $P < 0.05$; **, $P < 0.01$.

expression of FUT11 greatly reduced the PI3K/AKT pathway in GC cells. To uncover the molecular mechanism of FUT11 in GC cells, based on high-throughput sequencing analysis, we identified differentially expressed genes (DEGs) in stable knockdowns of FUT11 and control in AGS cells. We screened 201 DEGs based on LogFC≥1 and $P < 0.05$ (Table 1). And then analyzed DEGs for KEGG enrichment was found that PI3K-Akt signaling was the most significantly enriched pathway (Fig. 7a). Western blotting demonstrated that the inhibition of FUT11 significantly decreased the protein level of p-AKT and p-mTOR, while the protein level of PTEN was increased in GC cells (Fig. 7b–c).

3.6. Restoring the COL6A3 expression exhibited a reversal effect on FUT11 knockdown

To investigate if the PI3K/AKT pathway is implicated in the biological processes produced by FUT11, we utilized sh1-FUT11 and COL6A3 plasmids to restore COL6A3 expression in FUT11 knockdown cells (Fig. 8a–b). CCK-8 assay findings revealed that restoring COL6A3 expression significantly alleviated the suppressing effects of knockdown FUT11 on AGS and MKN-28 cell proliferation (Fig. 8c). Colony formation assay revealed that restoring COL6A3 expression significantly alleviated the suppressor effects of knockdown FUT11 colony formation ability of AGS and MKN-28 cells (Fig. 8d–e). Furthermore, transwell assay revealed that enhanced COL6A3 expression reverted FUT11 knockdown inhibitory effects on AGS and MKN-28 cell invasion (Fig. 8f–g).

4. Discussion

Gastric cancer (GC) is a malignancy that occurs with high frequency [16]. The World Health Organization reports that approximately one million new cases of GC are diagnosed annually [17]. Despite the development of an increasing number of diagnostic and treatment strategies for GC in recent years, the prognosis for patients remains poor [18]. Therefore, it is imperative to elucidate the molecular mechanisms underlying the occurrence and progression of GC.

Members including FUT1-11, POUT1, and POUT2 in the FUT family play as are enzymes involved in catalyzing the transference of fucose from GDP-fucose to glycoconjugates [19]. Since the FUT family members perform a vital function in a variety of cancer types, we discovered the key components of the FUT family that precipitate GC [20,21]. We discovered that of all the components of the FUT family, FUT11 was upmodulated in GC and that increased expression of FUT11 was a predictor of worse outcomes in GC patients utilizing bioinformatics analysis. As a result, we concentrated on the function of FUT11 expression in GC. The expression and importance of FUT11 have been extensively explored, as evidenced by prior research. Zhang et al. found that FUT11 exhibited a considerably elevated expression in gynecological cancer and that patients with greater FUT11 mRNA levels were expected to have a worse prognosis [22]. Zodro et al. reported that FUT11 was an essential biomarker that participates in the progression of clear cell

Table 1
All differently expressed genes (DEGs) between FUT11 knockdown group and and NC group were showed.

ID	log2(FC)	-log10 (pVal)
SLC12A4	3.0878973	0.000126721
NDST2	3.036394	6.13E-28
SSH1	3.0141063	0.000496093
FAM63B	2.9600845	1.81E-07
MRC2	2.9514865	3.70E-05
SAMD8	2.9151668	3.17E-15
LATS2	2.8580375	0.000129031
FKBP14	2.8522621	8.71E-05
MARVELD1	2.8364879	3.82E-08
OSBPL8	2.821377	1.93E-05
ARSB	2.7920784	5.40E-06
SUSD6	2.7811513	3.52E-07
FTX	2.7778453	7.29E-05
CDH11	2.7650571	0.000245087
CSGALNACT2	2.7618346	1.66E-24
MMP14	2.7337375	0.000109345
COL8A1	2.7195247	8.31E-07
NUAK1	2.7075191	5.77E-09
IFNAR1	2.7047424	6.32E-11
AFAP1	2.6797882	4.52E-05
MAP3K12	2.6605084	1.59E-05
KCTD10	2.6599368	8.41E-07
PHLDB1	2.6512572	3.91E-31
ITPRIPL2	2.6462487	3.08E-12
SEC22C	2.6312308	6.64E-49
ANXA7	2.6222568	6.80E-13
ZNF532	2.6153468	0.000163154
RP11-524D16_A.3	2.615218	4.40E-22
PDGFRB	2.6063509	0.000316794
MAP3K3	2.6023118	4.19E-09
ADGRA2	2.5998508	1.25E-08
ABL2	2.5780485	1.12E-11
TTBK2	2.5652532	3.01E-13
MAP4K5	2.5573699	5.32E-14
ARHGAP1	2.545213	3.87E-14
ZNF521	2.5371993	4.64E-09
COL5A1	2.5010498	2.08E-22
SH3PXD2A	2.4926397	2.00E-25
NAV1	2.4902336	1.91E-28
BICD2	2.4811606	1.37E-26
FAM160B1	2.4692647	3.25E-06
PURA	2.4688653	3.87E-20
REEP3	2.4485481	2.32E-08
FSTL1	2.4438322	2.64E-11
RUFY2	2.4412667	3.65E-05
BMPR2	2.3858126	3.05E-15
ZMIZ1	2.3856774	2.28E-07
QKI	2.3600429	3.37E-46
NOD1	2.3362155	3.84E-05
FBN1	2.3308615	1.03E-09
TIMP2	2.3108671	2.96E-09
RBFOX2	2.3021172	4.35E-07
PPP3CB	2.2991219	3.50E-08
SUFU	2.2929785	3.29E-06
WBP1L	2.2759331	3.24E-11
DNAJB14	2.2569975	4.02E-10
PLBD2	2.2515963	2.55E-14
SNX29	2.2484596	3.32E-05
FAM168A	2.2466698	0.000265729
HDAC7	2.2425232	0.000879469
KIRREL	2.2404304	1.17E-11
TCP11L1	2.2404023	6.99E-20
TBC1D2B	2.2347009	0.000224637
SPIN1	2.2262682	6.05E-09
ZBTB47	2.2234682	0.000145729
SNTB2	2.2195772	3.09E-06
PRRX1	2.201845	0.000260794

(*continued on next page*)

Table 1 (*continued*)

ID	log2(FC)	-log10 (pVal)
MSC-AS1	2.1894957	2.48E-18
MFAP3	2.1723403	2.30E-15
HEG1	2.1694847	3.90E-07
NDST1	2.1687848	0.000412011
DLG5	2.1653343	3.06E-10
RBSN	2.1649734	4.12E-08
SKI	2.1646013	3.23E-36
MORF4L1	2.1592502	3.41E-07
ACTR1A	2.1546173	3.44E-14
TCF4	2.1517073	1.31E-08
C16orf72	2.1450735	0.000456376
SNRK	2.1446871	3.77E-27
PEAK1	2.1382602	5.57E-15
DENND6A	2.1343822	2.78E-39
PLSCR4	2.1249448	5.48E-21
FBXL17	2.1115212	5.16E-10
COL6A2	2.1113889	1.32E-10
MAP3K2	2.108889	9.63E-08
KDM4B	2.1062305	8.12E-34
FZD1	2.1055321	0.000292715
RP11-815J21.4	2.1028599	8.16E-06
EVC	2.0376617	1.77E-14
PIGCP1	2.0230318	3.92E-15
LEPROT	2.0078516	2.56E-08
SNED1	−2.017496	1.04E-12
CHSY3	−2.025867	1.12E-21
FAM114A1	−2.026613	1.88E-09
BICC1	−2.04197	1.52E-07
RAB31	−2.046668	4.56E-13
SYDE1	−2.055408	2.15E-49
TMEM43	−2.061746	3.81E-22
SLC39A13	−2.080436	7.69E-11
SOCS5	−2.099787	5.97E-25
ARHGAP22	−2.100664	6.88E-29
C5orf24	−2.105759	8.11E-17
CALHM2	−2.110368	3.51E-34
SECISBP2L	−2.115369	3.44E-46
GPR68	−2.118772	0.000165477
AXL	−2.123348	5.67E-08
AFF4	−2.130034	6.06E-27
GINM1	−2.148049	5.02E-07
PXDN	−2.150816	0.000176132
ZFYVE1	−2.166804	3.82E-49
PPP2R5B	−2.174592	2.13E-16
ZNF490	−2.180858	1.86E-29
LTBP2	−2.189446	1.95E-34
COL5A2	−2.191624	1.16E-15
VCL	−2.202432	2.36E-05
SYNGAP1	−2.202653	0.000710874
GNA12	−2.203117	2.10E-13
RHOQ	−2.203554	4.57E-16
ZNF641	−2.205624	2.59E-07
SLAIN2	−2.234434	1.22E-31
PPM1F	−2.23755	0.000161056
SRPX2	−2.237823	1.81E-38
CASC4	−2.242747	9.64E-28
EVI5	−2.257592	7.93E-23
SEC24C	−2.271731	5.91E-10
TXNDC15	−2.283286	0.000469825
BMP8A	−2.304675	3.32E-53
ITGB1	−2.307293	1.01E-25
IDS	−2.308931	2.84E-23
THBS2	−2.329785	2.91E-61
COL3A1	−2.331483	9.97E-41
ANTXR1	−2.332839	5.03E-24
EHD2	−2.333941	0.000848521
LIMS1	−2.360753	5.10E-18
RUSC2	−2.362715	1.63E-47
SRGAP2	−2.386775	2.03E-12

(*continued on next page*)

Table 1 (*continued*)

ID	log2(FC)	-log10 (pVal)
AKAP2	−2.395605	0.000261254
BTBD19	−2.400124	1.74E-05
SGTB	−2.409809	0.00070843
DDX6	−2.416314	3.87E-46
HIC1	−2.417763	3.03E-38
MSANTD3	−2.435061	0.000266631
MAP4	−2.439247	1.36E-26
SNX18	−2.440412	6.30E-71
TMX2P1	−2.473948	3.88E-70
PLXDC2	−2.474335	1.69E-39
SH3PXD2B	−2.475142	6.35E-38
NLGN2	−2.481291	3.24E-09
ZYG11B	−2.494312	0.000231097
EDNRA	−2.497162	0.000263054
ARHGAP31	−2.509214	1.74E-39
LAMA4	−2.519783	9.44E-61
HIVEP2	−2.538376	7.44E-56
TGFB1	−2.547051	1.99E-15
PLEKHO2	−2.559899	8.21E-06
DYNC1LI2	−2.561195	1.45E-35
GRK4	−2.565037	2.23E-12
XIAP	−2.572249	1.03E-21
ATP8B2	−2.6032	4.13E-16
TWSG1	−2.626082	1.29E-12
FGD5-AS1	−2.63995	7.53E-09
AP3M1	−2.644592	4.52E-19
LBH	−2.670584	1.11E-06
BEND3P3	−2.67563	1.78E-06
KCTD20	−2.677744	1.14E-19
PRICKLE1	−2.682587	3.93E-07
MORF4L1P1	−2.708777	9.11E-11
GLI2	−2.739245	0.000100705
DCHS1	−2.740403	0.000132859
LRCH3	−2.742431	1.33E-26
PALM2-AKAP2	−2.756736	8.31E-15
DPP8	−2.777316	1.17E-11
RAPGEF1	−2.82806	3.41E-11
RP11-672A2.4	−2.83397	4.27E-14
ZNF500	−2.835574	8.54E-11
PHF21A	−2.84606	1.53E-34
PKD2	−2.852809	4.70E-38
TSPAN14	−2.85305	8.06E-10
NR3C1	−2.854894	1.85E-08
CSRNP2	−2.871222	5.27E-16
INPP5F	−2.872552	1.80E-12
VSTM4	−2.897104	1.14E-77
C1R	−2.951464	1.03E-73
KRBA2	−2.957003	1.07E-59
EPN2	−2.979667	3.66E-05
FAM134C	−3.075314	2.53E-50
ENTPD1	−3.116663	7.60E-23
CREBRF	−3.191824	3.76E-06
ZEB2	−3.221176	4.89E-44
NUMBL	−3.251947	6.68E-44
ITGAV	−3.371883	6.37E-16
SEMA4C	−3.378948	3.87E-55
IL1R1	−3.442762	2.12E-39
FTO	−3.590236	0.000665455
GOLGA3	−3.590608	4.90E-23
FCHSD2	−3.598777	1.33E-13
VPS39	−3.616467	4.80E-20
MEF2A	−3.616731	1.03E-15
RP11-752L20.3	−3.665705	1.40E-10
COL6A3	−3.673019	2.39E-09

renal cell carcinoma [23]. The present study delved deeper into the involvement of FUT11 in gastric cancer (GC). Our findings indicate that FUT11 expression levels were significantly elevated in GC tissues compared to adjacent tissues, and that FUT11 exhibits considerable diagnostic potential in distinguishing GC tissues from adjacent tissues.

Cao et al. exhibited that knockdown FUT11 expression promoted pancreatic cancer cell proliferation and metastasis via

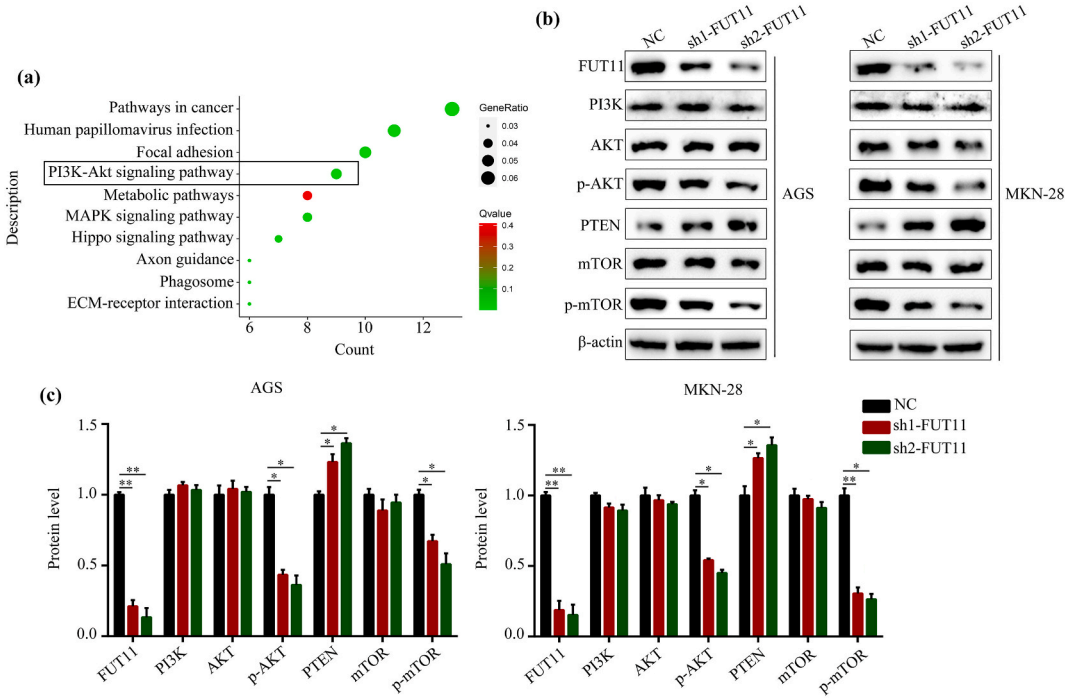

Fig. 7. Knockdown of FUT11 inhibited the activation of PI3K/AKT pathway. (a) Significant pathway which FUT11 enriched in was showed based on KEGG analysis. (b) The expression of PI3K, AKT, p-AKT, PTEN, mTOR and p-mTOR in negative control group and FUT11 knockdown cell. (c) Statistical plot of Western blot of assay. *, $P < 0.05$; **, $P < 0.01$.

maintaining stability pyruvate dehydrogenase kinase 1 [24] Ruan et al. revealed that knockdown of FUT11 decreased proliferation, colony formation, and invasion of hepatocellular carcinoma [25]. Additionally, we found that inhibition of FUT11 significantly reduced GC cell proliferation and motility. Futhermore, TCGA database and Pearson correlation analysis found that FUT11 was co-expressed with COL6A3 in GC tissues. COL6A3 is responsible for encoding the alpha-3 chain of type VI collagen, which is one of the three alpha chains that comprise type VI collagen [26]. Type VI collagen is a trimeric protein consisting of three distinct alpha chains: alpha-1(VI), alpha-2(VI), and alpha-3(VI) [27]. This protein is widely distributed throughout the extracellular matrix and can be found in various connective tissues, such as muscle, skin, tendon, and vessels [28]. Recent research has demonstrated that type VI collagen plays a crucial role in suppressing apoptosis and oxidative damage, regulating metabolic processes, and promoting cell growth [29,30]. High-throughput sequencing analysis of DEGs after FUT11 knockdown, and KEGG enrichment showed that PI3K-Akt signaling pathway was the most significantly enriched pathway. Futhermore, western blotting demonstrated that the inhibition of FUT11 significantly decreased the protein level of p-AKT and p-mTOR, while the protein level of PTEN was increased in GC cells. During tumor development, the PI3K/AKT signaling pathway was associated to the COL6A3 [31,32]. Ao et al. exhibited that silencing of COL6A3 suppressed GC cell proliferation, migration, and invasion and at the same time enhancing apoptosis via the PI3K/AKT signaling pathway [33]. Guo et al. reported that COL6A3 enhanced osteosarcoma cellular malignancy by triggering the PI3K/AKT pathway [34]. Futhermore, the inhibitory effects of FUT11 knockdown on cell proliferation and motility may be reversed by restoring COL6A3 expression in GC.

In summary, our study has demonstrated a negative correlation between the upregulation of FUT11 in gastric cancer (GC) tissues and the high expression of COL6A3. Our findings suggest that FUT11 can impede the onset and progression of GC via COL6A3 to regulate downstream PI3K-Akt signaling. Consequently, our research provides a novel biomarker for the diagnosis, and treatment of GC. However, the overall information about the association between FUT11 and GC risk was few. Thus, a larger sample size and more in depth analyses will be needed to verify the above results.

5. Conclusion

FUT11 promoted the GC proliferation, migration and invasion via the PI3K/AKT pathway.

Ethics approval and consent to participate

This study was reviewed and approved by the Medical Ethics Committee of Guizhou Medical University, Guiyang, China (approval number: 2200045). All animal studies were approved by the Institutional Animal Care and Use Committee of Committee of Guizhou Medical University.

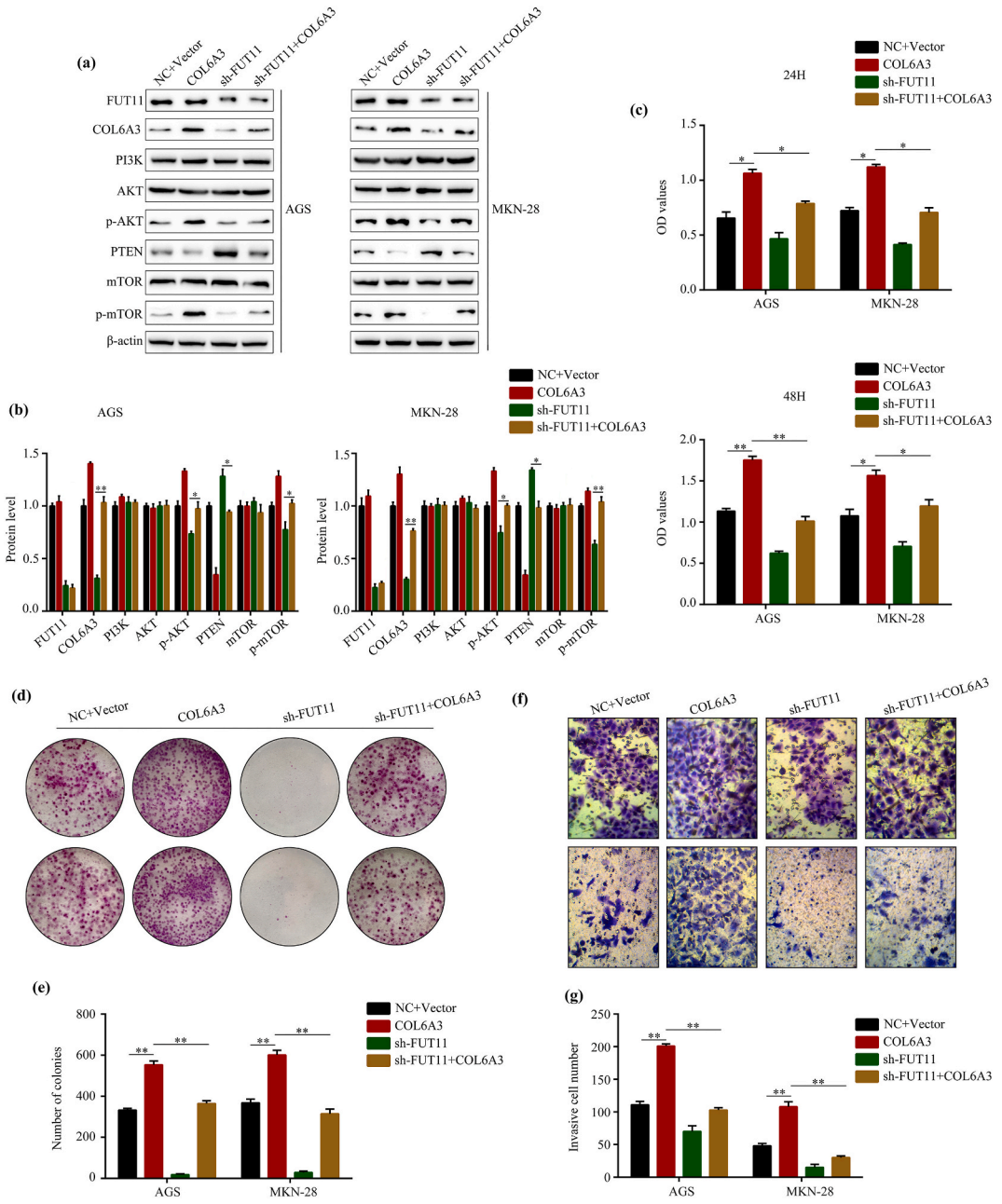

Fig. 8. Restored the expression of COL6A3 reversed the effects of FUT11 knockdown. GC cells were divided into three group according to the treatments: negative control (NC) + vector. FUT11 knockdown (sh-FUT11) + vector and sh- FUT11 + COL6A3 overexpression (COL6A3). (a) Western blot was used to detect the expression of COL6A3 and FUT11 in each group. (b) Statistical plot of Western blot of assay. (c) CCK-8 was used to detect the proliferation in each group. (d) Colony formation was used to detect the colony formation ability in each group. (e) Statistical plot of colony formation of assay. (f) Transwell assay was used to detect invasion in each group. (g) Statistical plot of transwell assay of assay. *, $P < 0.05$; **, $P < 0.01$.

Consent for publication

All authors have agreed to publish this manuscript.

Authors' contributions

Shan Lei: Conceived and designed the experiments; Wrote the paper.

Wenpeng Cao: Conceived and designed the experiments; Performed the experiments.
Yushi Yang; Jinzhi Lan: Performed the experiments; Analyzed and interpreted the data; Wrote the paper.
Zhirui Zeng: Analyzed and interpreted the data.
Min Lu: Contributed reagents, materials, analysis tools or data.

Data availability statement

No data was used for the research described in the article.

Declaration of competing interest

The authors declare that they have no known competing financial interests or personal relationships that could have appeared to influence the work reported in this paper.

Acknowledgments

This work was supported by Guizhou Medical University National Natural Science Foundation cultivation project (grant no. 20NSP020 and 19NSP034).

Appendix A. Supplementary data

Supplementary data to this article can be found online at https://doi.org/10.1016/j.heliyon.2023.e17600.

References

[1] M. Alsina, V. Arrazubi, M. Diez, J. Tabernero, Current developments in gastric cancer: from molecular profiling to treatment strategy, Nat. Rev. Gastroenterol. Hepatol. 20 (2023) 155–170.
[2] D.B. Hoffman, E.K. Nakakura, Laparoscopic gastrectomy for gastric cancer, JAMA Surg. 158 (2023) 454–455.
[3] R.J. Huang, M. Laszkowska, H. In, J.H. Hwang, M. Epplein, Controlling gastric cancer in a world of heterogeneous risk, Gastroenterology 164 (2023) 736–751.
[4] S. Li, W. Yu, F. Xie, H. Luo, Z. Liu, W. Lv, D. Shi, D. Yu, P. Gao, C. Chen, et al., Neoadjuvant therapy with immune checkpoint blockade, antiangiogenesis, and chemotherapy for locally advanced gastric cancer, Nat. Commun. 14 (2023) 8.
[5] Q. Leng, J.H. Tsou, M. Zhan, F. Jiang, Fucosylation genes as circulating biomarkers for lung cancer, J. Cancer Res. Clin. Oncol. 144 (2018) 2109–2115.
[6] R. Fan, X. Han, Y. Gong, L. He, Z. Xue, Y. Yang, L. Sun, D. Fan, Y. You, F. Meng, et al., Alterations of fucosyltransferase genes and fucosylated glycans in gastric epithelial cells infected with Helicobacter pylori, Pathogens 10 (2021).
[7] F. Wu, Y. Qin, Q. Jiang, J. Zhang, F. Li, Q. Li, X. Wang, Y. Gao, J. Miao, C. Guo, et al., MyoD1 suppresses cell migration and invasion by inhibiting FUT4 transcription in human gastric cancer cells, Cancer Gene Ther. 27 (2020) 773–784.
[8] M. Padro, L. Cobler, M. Garrido, C. de Bolos, Down-regulation of FUT3 and FUT5 by shRNA alters Lewis antigens expression and reduces the adhesion capacities of gastric cancer cells, Biochim. Biophys. Acta 1810 (2011) 1141–1149.
[9] S. Dong, Z. Wang, B. Huang, J. Zhang, Y. Ge, Q. Fan, Z. Wang, Bioinformatics insight into glycosyltransferase gene expression in gastric cancer: POFUT1 is a potential biomarker, Biochem. Biophys. Res. Commun. 483 (2017) 171–177.
[10] Z. Tang, C. Li, B. Kang, G. Gao, C. Li, Z. Zhang, GEPIA: a web server for cancer and normal gene expression profiling and interactive analyses, Nucleic Acids Res. 45 (2017) W98–W102.
[11] N. Gao, J. Liu, D. Liu, Y. Hao, L. Yan, Y. Ma, H. Zhuang, Z. Hu, J. Gao, Z. Yang, et al., c-Jun transcriptionally regulates alpha 1, 2-fucosyltransferase 1 (FUT1) in ovarian cancer, Biochimie 107 Pt B (2014) 286–292.
[12] N. Li, Y. Liu, Y. Miao, L. Zhao, H. Zhou, L. Jia, MicroRNA-106b targets FUT6 to promote cell migration, invasion, and proliferation in human breast cancer, IUBMB Life 68 (2016) 764–775.
[13] L. Liang, C. Gao, Y. Li, M. Sun, J. Xu, H. Li, L. Jia, Y. Zhao, miR-125a-3p/FUT5-FUT6 axis mediates colorectal cancer cell proliferation, migration, invasion and pathological angiogenesis via PI3K-Akt pathway, Cell Death Dis. 8 (2017) e2968. 10.
[14] M. Jurikova, L. Danihel, S. Polak, I. Varga, Ki67, PCNA, and MCM proteins: markers of proliferation in the diagnosis of breast cancer, Acta Histochem. 118 (2016) 544–552.
[15] W. Strzalka, A. Ziemienowicz, Proliferating cell nuclear antigen (PCNA): a key factor in DNA replication and cell cycle regulation, Ann. Bot. 107 (2011) 1127–1140.
[16] Y. Lu, Z. Jin, J. Hou, X. Wu, Z. Yu, L. Yao, T. Pan, X. Chang, B. Yu, J. Li, et al., Calponin 1 increases cancer-associated fibroblasts-mediated matrix stiffness to promote chemoresistance in gastric cancer, Matrix Biol. 115 (2023) 1–15.
[17] S. Ma, M. Zhou, Y. Xu, X. Gu, M. Zou, G. Abudushalamu, Y. Yao, X. Fan, G. Wu, Clinical application and detection techniques of liquid biopsy in gastric cancer, Mol. Cancer 22 (2023) 7.
[18] A.P. Thrift, T.N. Wenker, H.B. El-Serag, Global burden of gastric cancer: epidemiological trends, risk factors, screening and prevention, Nat. Rev. Clin. Oncol. 20 (2023) 338–349.
[19] A. Blanas, L.A.M. Cornelissen, M. Kotsias, J.C. van der Horst, H.J. van de Vrugt, H. Kalay, D.I.R. Spencer, R.P. Kozak, S.J. van Vliet, Transcriptional activation of fucosyltransferase (FUT) genes using the CRISPR-dCas9-VPR technology reveals potent N-glycome alterations in colorectal cancer cells, Glycobiology 29 (2019) 137–150.
[20] K. Bastian, E. Scott, D.J. Elliott, J. Munkley, FUT8 alpha-(1,6)-fucosyltransferase in cancer, Int. J. Mol. Sci. 22 (2021).
[21] K. Tada, M. Ohta, S. Hidano, K. Watanabe, T. Hirashita, Y. Oshima, A. Fujnaga, H. Nakanuma, T. Masuda, Y. Endo, et al., Fucosyltransferase 8 plays a crucial role in the invasion and metastasis of pancreatic ductal adenocarcinoma, Surg. Today 50 (2020) 767–777.
[22] X. Zhang, Y. Wang, Identification of hub genes and key pathways associated with the progression of gynecological cancer, Oncol. Lett. 18 (2019) 6516–6524.
[23] E. Zodro, M. Jaroszewski, A. Ida, T. Wrzesinski, Z. Kwias, H. Bluyssen, J. Wesoly, FUT11 as a potential biomarker of clear cell renal cell carcinoma progression based on meta-analysis of gene expression data, Tumour Biol. 35 (2014) 2607–2617.
[24] W. Cao, Z. Zeng, R. Pan, H. Wu, X. Zhang, H. Chen, Y. Nie, Z. Yu, S. Lei, Hypoxia-related gene FUT11 promotes pancreatic cancer progression by maintaining the stability of PDK1, Front. Oncol. 11 (2021), 675991.

[25] W. Ruan, Y. Yang, Q. Yu, T. Huang, Y. Wang, L. Hua, Z. Zeng, R. Pan, FUT11 is a target gene of HIF1alpha that promotes the progression of hepatocellular carcinoma, Cell Biol. Int. 45 (2021) 2275–2286.
[26] E. Choi, S. Shin, S. Lee, S.J. Lee, J. Park, Coexistence of digenic mutations in the collagen VI genes (COL6A1 and COL6A3) leads to Bethlem myopathy, Clin. Chim. Acta 508 (2020) 28–32.
[27] C.Y. Kang, J. Wang, D. Axell-House, P. Soni, M.L. Chu, G. Chipitsyna, K. Sarosiek, J. Sendecki, T. Hyslop, M. Al-Zoubi, et al., Clinical significance of serum COL6A3 in pancreatic ductal adenocarcinoma, J. Gastrointest. Surg. 18 (2014) 7–15.
[28] Y. Shi, X. Wu, J. Zhou, W. Cui, J. Wang, Q. Hu, S. Zhang, L. Han, M. Zhou, J. Luo, et al., Single-nucleus RNA sequencing reveals that decorin expression in the amygdala regulates perineuronal nets expression and fear conditioning response after traumatic brain injury, Adv. Sci. 9 (2022), e2104112.
[29] G. Lin, R. Zhao, Y. Wang, J. Han, Y. Gu, Y. Pan, C. Ren, S. Ren, C. Xu, Dynamic analysis of N-glycomic and transcriptomic changes in the development of ovarian cancer cell line A2780 to its three cisplatin-resistant variants, Ann. Transl. Med. 8 (2020) 289.
[30] Y. Tong, P.S.W. Cheng, C.S. Or, S.S.K. Yue, H.C. Siu, S.L. Ho, S.Y.K. Law, W.Y. Tsui, D. Chan, S. Ma, et al., Escape from cell-cell and cell-matrix adhesion dependence underscores disease progression in gastric cancer organoid models, Gut 72 (2023) 242–255.
[31] Y. Wu, Y. Xu, Integrated bioinformatics analysis of expression and gene regulation network of COL12A1 in colorectal cancer, Cancer Med. 9 (2020) 4743–4755.
[32] P. Yan, Y. Wang, X. Meng, H. Yang, Z. Liu, J. Qian, W. Zhou, J. Li, Whole exome sequencing of ulcerative colitis-associated colorectal cancer based on novel somatic mutations identified in Chinese patients, Inflamm. Bowel Dis. 25 (2019) 1293–1301.
[33] R. Ao, L. Guan, Y. Wang, J.N. Wang, Silencing of COL1A2, COL6A3, and THBS2 inhibits gastric cancer cell proliferation, migration, and invasion while promoting apoptosis through the PI3k-Akt signaling pathway, J. Cell. Biochem. 119 (2018) 4420–4434.
[34] H.L. Guo, G. Chen, Z.L. Song, J. Sun, X.H. Gao, Y.X. Han, COL6A3 promotes cellular malignancy of osteosarcoma by activating the PI3K/AKT pathway, Rev. Assoc. Med. Bras. 66 (1992) (2020) 740–745.